



**UNIVERSITY OF LEEDS**

This is a repository copy of *Supraglacial Ponds Regulate Runoff From Himalayan Debris-Covered Glaciers*.

White Rose Research Online URL for this paper:  
<http://eprints.whiterose.ac.uk/124878/>

Version: Accepted Version

---

**Article:**

Irvine-Fynn, TDL, Porter, PR, Rowan, AV et al. (6 more authors) (2017) Supraglacial Ponds Regulate Runoff From Himalayan Debris-Covered Glaciers. *Geophysical Research Letters*, 44 (23). pp. 11894-11904. ISSN 0094-8276

<https://doi.org/10.1002/2017GL075398>

---

**Reuse**

Items deposited in White Rose Research Online are protected by copyright, with all rights reserved unless indicated otherwise. They may be downloaded and/or printed for private study, or other acts as permitted by national copyright laws. The publisher or other rights holders may allow further reproduction and re-use of the full text version. This is indicated by the licence information on the White Rose Research Online record for the item.

**Takedown**

If you consider content in White Rose Research Online to be in breach of UK law, please notify us by emailing [eprints@whiterose.ac.uk](mailto:eprints@whiterose.ac.uk) including the URL of the record and the reason for the withdrawal request.



[eprints@whiterose.ac.uk](mailto:eprints@whiterose.ac.uk)  
<https://eprints.whiterose.ac.uk/>

## Supraglacial ponds regulate runoff from Himalayan debris-covered glaciers

Tristram D.L. Irvine-Fynn<sup>1\*</sup>, Philip R. Porter<sup>2</sup>, Ann V. Rowan<sup>3</sup>, Duncan J. Quincey<sup>4</sup>,  
Morgan J. Gibson<sup>1</sup>, Jonathan W. Bridge<sup>5</sup>, C. Scott Watson<sup>4</sup>, Alun Hubbard<sup>1,6</sup>, Neil F.  
Glasser<sup>1</sup>

<sup>1</sup>Centre for Glaciology, Department of Geography and Earth Sciences, Aberystwyth University, Aberystwyth, UK. <sup>2</sup>Department of Biological and Environmental Sciences, University of Hertfordshire, Hatfield, UK. <sup>3</sup>Department of Geography, University of Sheffield, Sheffield, UK. <sup>4</sup>School of Geography, University of Leeds, Leeds, UK. <sup>5</sup>Department of the Natural and Built Environment, Sheffield Hallam University, Sheffield, UK. <sup>6</sup>Centre for Arctic Gas Hydrate, Environment and Climate, Department of Geosciences, The Arctic University of Norway, Tromsø, Norway.

\* Corresponding author: Tristram Irvine-Fynn ([tdi@aber.ac.uk](mailto:tdi@aber.ac.uk))

### Key Points:

- The monsoon season runoff hydrograph from Khumbu Glacier displays progressive changes in diurnal timing and recession characteristics.
- We propose that observed hydrological behavior results from seasonal evolution of supraglacial ponds and connections.
- Predicted expansion of debris-covered areas and pond extents will influence downstream timing, availability and quality of meltwater in the Himalaya.

## Abstract

1 Meltwater and runoff from glaciers in High Mountain Asia is a vital freshwater resource for one  
2 fifth of the Earth's population. Between 13% and 36% of the region's glacierized areas exhibit  
3 surface debris cover and associated supraglacial ponds whose hydrological buffering roles  
4 remain unconstrained. We present a high-resolution meltwater hydrograph from the extensively  
5 debris-covered Khumbu Glacier, Nepal, spanning a seven-month period in 2014. Supraglacial  
6 ponds and accompanying debris cover modulate proglacial discharge by acting as transient and  
7 evolving reservoirs. Diurnally, the supraglacial pond system may store >23% of observed mean  
8 daily discharge, with mean recession constants ranging from 31 to 108 hours. Given projections  
9 of increased debris-cover and supraglacial pond extent across High Mountain Asia, we conclude  
10 that runoff regimes may become progressively buffered by the presence of supraglacial  
11 reservoirs. Incorporation of these processes is critical to improve predictions of the region's  
12 freshwater resource availability and cascading environmental effects downstream.

13

## 14 **1 Introduction**

15 An estimated 1.4 billion people depend on freshwater sourced from snow and ice melt in High  
16 Mountain Asia [*Immerzeel et al.*, 2010]. Although highly variable across the region, this  
17 meltwater typically contributes between 20% and 50% of the total annual runoff [*Bookhagen and*  
18 *Burbank*, 2010; *Immerzeel and Bierkens*, 2012; *Lutz et al.*, 2014]. Contemporary observations  
19 [*Bolch et al.*, 2012; *Kaab et al.*, 2012; *Pritchard*, 2017; *Brun et al.*, 2017] and predicted trends  
20 [e.g. *Shea et al.*, 2015a; *Soncini et al.*, 2016] of glaciers in the Himalaya demonstrate declining  
21 ice volumes, but highlight uncertainty over the associated glacio-hydrological impacts and  
22 consequent water stress arising from climate change. One important cause of this ambiguity is  
23 the presence of a supraglacial debris mantle present on many of the region's glaciers, which  
24 covers up to 36% of the glacierized area in the Everest region [*Bolch et al.*, 2012; *Kaab et al.*,  
25 2012; *Scherler et al.*, 2011; *Thakuri et al.*, 2014]. This debris mantle commonly causes  
26 downglacier ablation areas to exhibit low surface gradients and velocities [e.g. *Quincey et al.*  
27 2007; *Scherler et al.*, 2011; *Thompson et al.*, 2016; *Salerno et al.*, 2017] and its overall extent is  
28 increasing and predicted to expand further [*Rowan et al.*, 2015; *Thakuri et al.*, 2014; *Bolch et al.*,  
29 2008]. Supraglacial debris exerts a critical influence on glacier response to climate forcing  
30 because, dependent on its thickness, debris can either accelerate or retard ablation [*Østrem* 1959;  
31 *Evatt et al.*, 2015]. This effect, coupled with the dynamic topography of the glacier surface,  
32 promotes highly heterogenous ablation and the formation of surface lakes and ponds, which are a  
33 common feature of receding debris-covered glaciers [*Reynolds*, 2000; *Benn et al.*, 2012;  
34 *Gardelle et al.*, 2011; *Watson et al.*, 2016; *Bassnet et al.*, 2013; *Miles et al.*, 2016, 2017a,b;  
35 *Narama et al.*, 2017]. However, the processes and causal relationships underpinning the spatial  
36 distribution of supraglacial ponds remain unclear [*Salerno et al.*, 2017].

37 Supraglacial ponds are 'hotspots' of glacier ablation [*Mertes et al.*, 2016] due to their reflective  
38 and thermal characteristics [*Sakai et al.*, 2000; *Benn et al.*, 2001; *Miles et al.*, 2016; *Watson et*  
39 *al.*, 2017a] and the presence of bare-ice cliffs associated with pond formation and growth [*Sakai*  
40 *et al.*, 2002; *Brun et al.*, 2016; *Watson et al.*, 2017b]. Consequently, ponds may accelerate glacier  
41 thinning and recession and act as temporary meltwater storage reservoirs [*Benn et al.*, 2001,  
42 2012]. Ponds on debris-covered glaciers are commonly either transient features due to inception  
43 or collapse of near-surface or shallow englacial drainage routes and consequent drainage, or

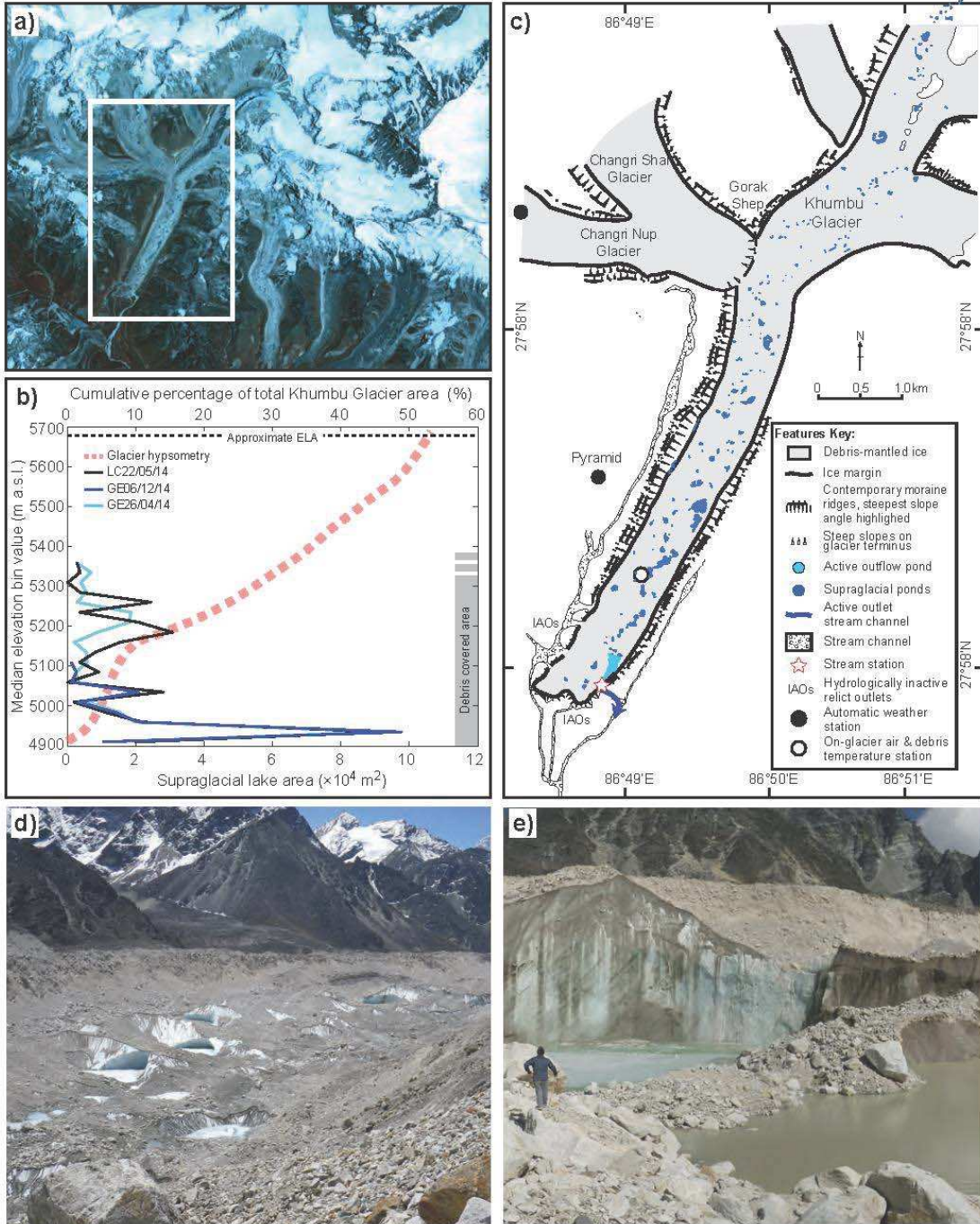
44 appear ‘perched’ in closed basins where efficient flowpaths are absent [Reynolds, 2000; Benn et  
45 al., 2001; Miles et al., 2017b; Watson et al., 2017a]. Seasonally, ponds on Himalayan glaciers  
46 typically grow both in area and depth [Watson et al., 2017a], attaining maximum extent mid-  
47 monsoon and declining in size thereafter [Miles et al., 2017a; Narama et al., 2017; Watson et al.,  
48 2016]. Inter-annually, debris redistribution and change in surface topography results in variation  
49 in pond positions [Narama et al., 2017; Watson et al., 2016] and as ponds attain their local  
50 hydrological base-level they may evolve into larger scale lakes [Thompson et al., 2016; Mertes et  
51 al., 2016]. Observations of supraglacial pond water quality confirm that hydrological linkages do  
52 exist between ponds [Takeuchi et al., 2000; Bhatt et al., 2016], and pond extent may be governed  
53 by the evolving development and (re)organization of supraglacial drainage systems [Watson et  
54 al., 2016, 2017a; Miles et al., 2017b]. Yet the extent to which these ponds impact upon  
55 meltwater generation and modify the seasonal hydrograph remains poorly quantified.

56 A lack of *in situ* observations of meltwater generation, transit and runoff for Himalayan glaciers  
57 [Immerzeel et al., 2012; Bajracharya et al., 2015] has led to uncertainties in the prediction of  
58 their hydrological response to environmental forcing. For example, some numerical models of  
59 debris-covered glacier systems utilize a linear reservoir parameterization linking proglacial  
60 discharge to meltwater production [e.g. Ragettli et al., 2015; Fujita and Sakai, 2014]. Such  
61 methods though fail to account for the potential hydrological complexities in the region.  
62 Specifically, the presence of interconnected supraglacial ponds implies a potentially complex  
63 hydrological system [Miles et al., 2017b] that will modulate the water inputs to, and outputs from  
64 the glacier system. Hence, the acquisition of detailed measurements characterizing the  
65 hydrological behavior of debris-covered glaciers on diurnal to seasonal timescales is an  
66 imperative for improved predictions of meltwater delivery to downstream water resources  
67 throughout the Himalaya. Here, we present the results of a glacier-scale runoff monitoring  
68 program at the debris-covered Khumbu Glacier in the Everest region of Nepal. Our  
69 measurements span a 190-day period from April to November 2014 including the summer  
70 monsoon season.

## 71 **2 Field Site and Methods**

72 Khumbu Glacier (27.97°N, 86.83°E) flows from the southern flanks of Mount Everest to its  
73 terminus at ~4900 m a.s.l. (Figure 1a). The terminus elevation is slightly lower than the local

74 permafrost limit of ~5000 m a.s.l. [Schmid *et al.*, 2015]. The glacier is likely to be polythermal,  
75 with an estimated 17 m deep cold surface ice layer [Mae *et al.*, 1975]. The glacier thinned at  
76 approximately  $-0.6 \text{ m a}^{-1}$  between 2000 and 2015, with losses of  $-1.4 \text{ m a}^{-1}$  at elevations of  
77 5200–5300 m [King *et al.*, 2017]. Approximately 47% of the 41 km<sup>2</sup> glacier including the  
78 Changri Nup and Changri Shar tributaries is debris-covered (Figure 1b). Supraglacial debris  
79 thickness varies from 0.1 m to over 3 m and is concentrated over the lowermost 8 km of the  
80 glacier [Soncini *et al.*, 2016], overlying 20 m to 440 m of glacier ice [Gades *et al.*, 2000]. Recent  
81 observations [e.g. Nuimura *et al.*, 2011] indicate that this debris cover has become increasingly  
82 topographically uneven: differential ablation has resulted in a complex glacier surface  
83 characterized by the presence of numerous supraglacial water bodies [Wessels *et al.*, 2002;  
84 Watson *et al.*, 2016]. Throughout 2014, ~1% of the total debris-covered area comprised  
85 supraglacial ponds (Figures 1b-e). However, as elsewhere in the region, the hydrological  
86 evolution and connectivity of these supraglacial ponds is poorly constrained. The Changri Nup  
87 and Changri Shar tributaries are now physically disconnected, but retain a surface hydrological  
88 connection with the Khumbu Glacier tongue [Vincent *et al.*, 2016]. The only visible source of  
89 meltwater runoff flowing from the Khumbu catchment emerges from a turbid supraglacial lake  
90 situated close to the eastern glacier margin (Figure 1c). There is no evidence of alternative,  
91 active terminal or lateral outlets for englacial or subglacial drainage pathways. Runoff data were  
92 recorded immediately downstream of this outlet lake, where meltwater drains via a breach in the  
93 eastern Little Ice Age lateral moraine to the upper Dudh Koshi.



94 **Figure 1:** (a) ASTER imagery (Sept 2012) of the Everest region, Nepal, outlining lower  
95 elevations of the Khumbu Glacier detailed in (c); (b) hypsometry and supraglacial pond area in  
96 Khumbu Glacier ablation zone based on satellite imagery from 26 April, 22 May and 6  
97 December 2014 [see *Watson et al.*, 2016]; (c) ablation zone of Khumbu Glacier highlighting key  
98 data collection sites and major geomorphological features, including hydrologically inactive  
99 outlets (IAOs) indicative of abandoned drainage routes and supraglacial lake positions on 26  
100 April 2014 prior to the onset of the monsoon season; (d, e) oblique images illustrating typical  
101 debris cover and pond morphology, taken during the pre-monsoon period, May 2014.

102

103 Discharge (Q) data were collected between 14 May and 12 November (Day of Year (DOY) 135  
104 to 317) using standard methods [*Herchy*, 1995]. A hydrological monitoring station was  
105 established in a stable reach of the sole outflow channel at 4930 m a.s.l.. Average water stage  
106 was recorded at 30 min intervals using a Druck PDCR1730 pressure transducer and Campbell  
107 Scientific (CS) CR1000 data logger. A stage-discharge rating curve was developed using  
108 triplicate dilutions [*Hudson and Fraser*, 2005] of 3 mL aliquots of 10% fluorescein and a Turner  
109 Designs Cyclops7 fluorometer linked to a CS CR10X datalogger. A non-linear stage-discharge  
110 relationship yielded a coefficient of determination of  $r^2 = 0.79$  ( $n = 18$ ). Estimated uncertainty in  
111 Q is <15%, although this is increased for higher Q values [see *Supplementary Information; Rantz*  
112 *et al.*, 1982; *Sakai et al.*, 1997; *DiBaldassarre and Montanari*, 2009]. On-glacier air temperature  
113 ( $T_a$ ) and debris temperature ( $T_d$ ) were monitored at 4935 m a.s.l. using Gemini TinyTag2 logging  
114 thermistors with a stated measurement accuracy of  $\pm 0.4^\circ\text{C}$  (Figure 1c). The  $T_a$  sensor was  
115 mounted in a naturally aspirated radiation shield 1 m above the debris surface; the  $T_d$  sensors  
116 were located within the debris layer at depths of 0.55 and 1.0 m below the surface and away from  
117 the debris-ice interface. All temperature measurements were recorded at 30-min intervals. Local  
118 incident shortwave radiation ( $SW_{in}$ ) was recorded at an automatic weather station 5363 m a.s.l.  
119 on the Changri Nup Glacier (Figure 1c) using a Kipp & Zonen CNR4 sensor with 3%  
120 uncertainty. Precipitation (P) was measured at Pyramid Observatory (Figure 1c) at 5035 m a.s.l.  
121 using a Geonor T-200 gauge; these hourly data were corrected for undercatch of solid  
122 precipitation and have an estimated accuracy of  $\pm 15\%$  [*Sherpa et al.*, 2017].



123 We examined the timing of peak discharge and the shape of the diurnal hydrograph using  
 124 standard approaches; lag times between time-series were identified using a moving window  
 125 cross-correlation [e.g. *Jobard and Dzikowski, 2006*], while we classified diurnal hydrographs  
 126 using a paired Principal Components Analysis (PCA) and Hierarchical Cluster Analysis (HCA)  
 127 approach [e.g. *Hannah et al., 2000; Swift et al., 2005*]. Specifically, daily (24 hr) hydrographs  
 128 were assumed to commence at low Q at 06:00, PCA was conducted without rotation and only  
 129 components with eigenvalues > 1.0 were retained. PCA identified modes of diurnal Q variation  
 130 defined by the standardized component loadings and these loadings for each day were clustered  
 131 using Euclidean distance measures and a within-groups linkage method. A total of 6 groups were  
 132 identified and further classified using a second, independent HCA that defined diurnal  
 133 hydrograph similarity based on key discharge metrics following z-score normalization. Daily  
 134 hydrographs were then described based on ‘shape’ defined by PCA clusters and ‘magnitude’  
 135 identified in the secondary HCA.

136 Estimates of recession storage constants (K) for each diurnal hydrograph were derived from  
 137 semi-logarithmic plots of Q versus time [e.g. *Gurnell, 1993; Hodgkins et al., 2013*] where:

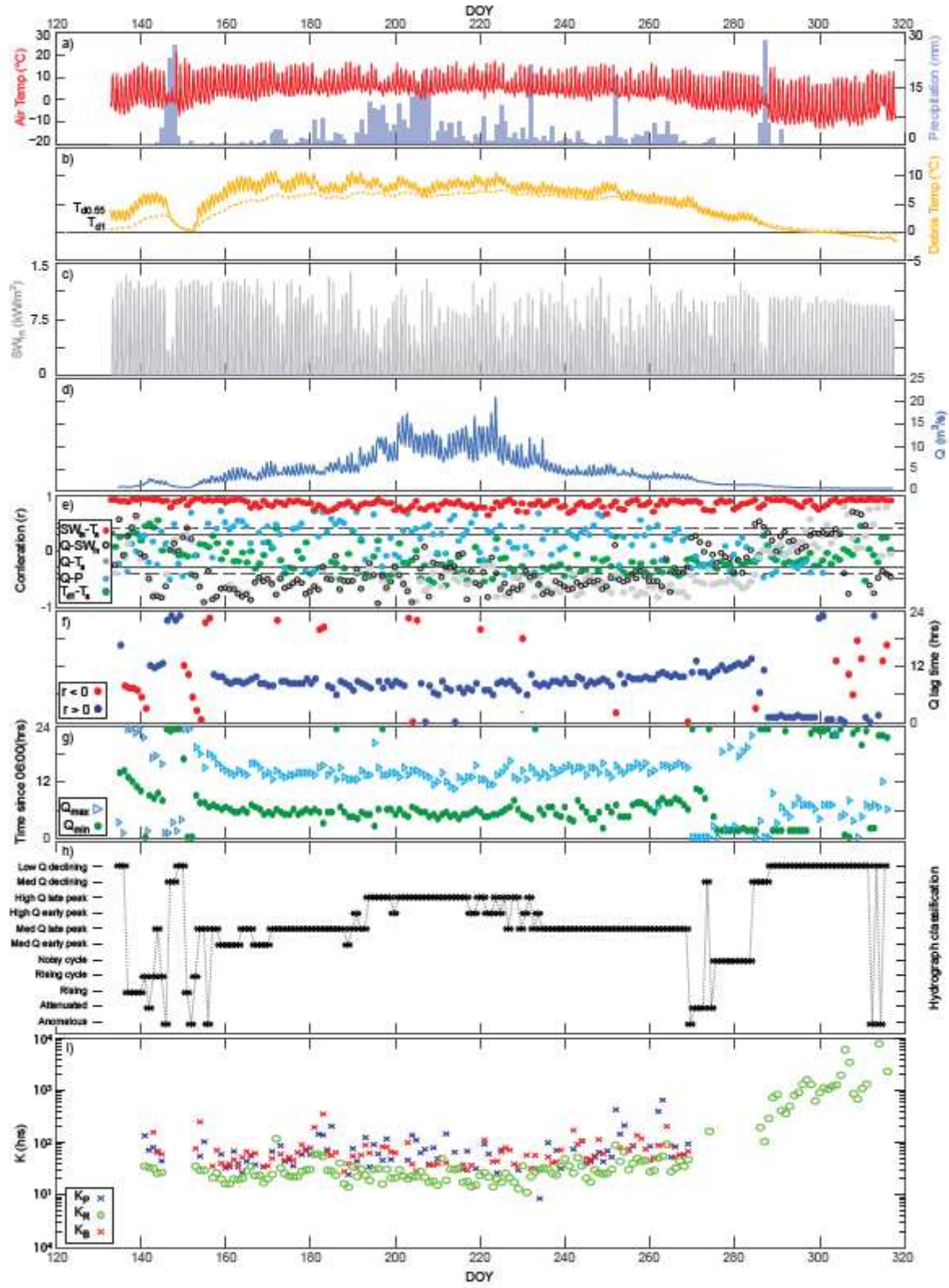
$$138 \quad \mathbf{K} = \frac{-t}{\ln\left(\frac{Q_t}{Q_0}\right)} \quad \text{Eq.1}$$

139 for which  $t$  is time since the start of the recession segment, and  $Q_0$  and  $Q_t$  the discharge at the  
 140 start of the recession segment and at time  $t$ , respectively. For all days classified as exhibiting  
 141 diurnal discharge cycles ( $n = 117$ ) or constant recessional hydrographs ( $n = 29$ ), K-values were  
 142 calculated from the time-step following peak discharge, or from 18:00 in the case of persistent  
 143 recession hydrographs. Recession segments and associated aggregate recession constants were  
 144 identified using segmented linear regression for cases exhibiting durations >1 hr.

### 145 **3 Results**

146 The meteorological and discharge time-series (Figure 2a-d) for the 2014 monsoon season reveal  
 147 that  $T_a$  and  $SW_{in}$  exhibited strong diurnal variations, with highest incident energy fluxes between  
 148 10:00 and 15:00, as typifies the region [see *Shea et al., 2015b*]. These two variables were highly  
 149 correlated over the diurnal cycle ( $r > 0.5$ ,  $p < 0.05$ ) throughout the observation period (Figure

150 2e). Seasonal changes in  $T_d$  aligned well with  $T_a$ , although at the daily timestep, correlation  
151 suggested a changing lag between variables (Figure 2e). Despite a distinct diurnal variability in  
152  $T_d$ , variation was suppressed at depth (Figure 2b), and  $T_d$  remained below  $0^\circ\text{C}$  following DOY  
153 300. The seasonal pattern of  $Q$  broadly followed that of  $T_a$  with an underlying diurnal fluctuation  
154 of between  $0.005$  and  $12.3 \text{ m}^3 \text{ s}^{-1}$ , and daily mean  $Q$  peaking at  $\sim 9 \text{ m}^3 \text{ s}^{-1}$  which compares well  
155 with published records of discharge during 2014 for the upper Dudh Koshi [*Soncini et al.*, 2016;  
156 see *Supplementary Information*]. Interestingly, diurnal correlation indicated  $Q$  and both  $T_a$  and  
157  $\text{SW}_{\text{in}}$  vary out of phase for much of the observation period (Figure 2e).  $Q$  lagged  $T_a$  progressively  
158 decreasing from 12 to 6 hrs until DOY 220, and subsequently returning to lags  $>12$  hrs until  
159 DOY 285 when lags dropped again to  $\sim 6$  hrs (Figure 2f). The diurnal hydrograph cycle became  
160 steadily delayed until DOY270 when  $T_d$  declined to  $\sim 5^\circ\text{C}$  and continued to fall when a  
161 protracted hydrograph recession dominated. While statistically significant diurnal correlations  
162 between  $Q$  and  $P$  were found, these were inconsistent and showed no systematic trend (Figure  
163 2e). Lag analysis highlighted statistically significant correlations ( $r > 0.405$ ,  $p < 0.05$ ) between  $Q$   
164 and  $P$  over 24 hr periods, predominantly with  $Q$  lagged by  $>10$  hrs, however no pattern in lag  
165 time was observed.



167 **Figure 2:** Time-series of (a) on-glacier air temperature  $T_a$  and total daily precipitation  $P$ , (b)  
 168 debris temperature  $T_d$  at 0.55 and 1.0 m below the debris surface, (c) incident shortwave  
 169 radiation  $SW_{in}$  and (d) meltwater discharge  $Q$ . Analyses identify (e) daily correlations between  
 170  $T_a$ ,  $SW_{in}$ ,  $P$  and  $Q$  with the 95% confidence levels indicated for the hourly ( $r \approx 0.41$ ) and half-  
 171 hourly ( $r \approx 0.29$ ) data sets, (f) the lag time between daily peak  $T_a$  and maximum  $Q$ , (g) the timing  
 172 of minimum and maximum  $Q$ , (h) the daily hydrograph classification based on shape and  
 173 magnitude, and (i) the three principal hydrograph recession constants ( $K_P$ ,  $K_R$  and  $K_B$ ).

174

175

176 Three sequential recession segments were identified as typical within the time-series: (i) slow  
 177 decrease in  $Q$  lasting  $\leq 7$  hours immediately following peak  $Q$  ( $K_P$ ), (ii) major recession  
 178 component of rapid decrease in  $Q$  over  $\sim 9$  hours duration ( $K_R$ ), and (iii) a second slow decrease  
 179 for  $\sim 5$  hours prior to the onset of the next diurnal cycle ( $K_B$ ). Where only a singular extended  
 180 recession was identified, this was taken to be  $K_R$ .  $K_P$  and  $K_B$  were found to be statistically  
 181 similar, but lacked a significant temporal trend, while  $K_R$  showed a strong non-linear association  
 182 with peak  $Q$ , decreasing and increasing as the monsoon season progressed. While aggregate  $K$ -  
 183 values broadly agree with the magnitude of those identified in other glacial runoff records (mean  
 184  $K_P = 86.7$  and  $K_B = 72.4$  hrs, while mean  $K_R = 108$  hrs for the season, but 31.1 hrs before  
 185 DOY270), the recession segment pattern contrasts with the commonly reported systematic  
 186 increase in  $K$ -values over diurnal hydrograph recession segments [e.g. *Gurnell, 1993; Hodgkins*  
 187 *et al., 2013*]. No association between  $K$ -values and  $P$  or daily peak  $Q$  was found. In tests,  
 188 uncertainty related to the rating curve used to derive the  $Q$  time-series [see *Supplementary*  
 189 *Information; Rantz et al., 1982*] did not impact the recession patterns identified; however, if  
 190 using a power-law rating curve [*Herchy, 1995*], recession constants  $K_P$ ,  $K_R$  and  $K_B$  increased by  
 191  $81 \pm 30\%$ ,  $51 \pm 50\%$  and  $57 \pm 26\%$  respectively.

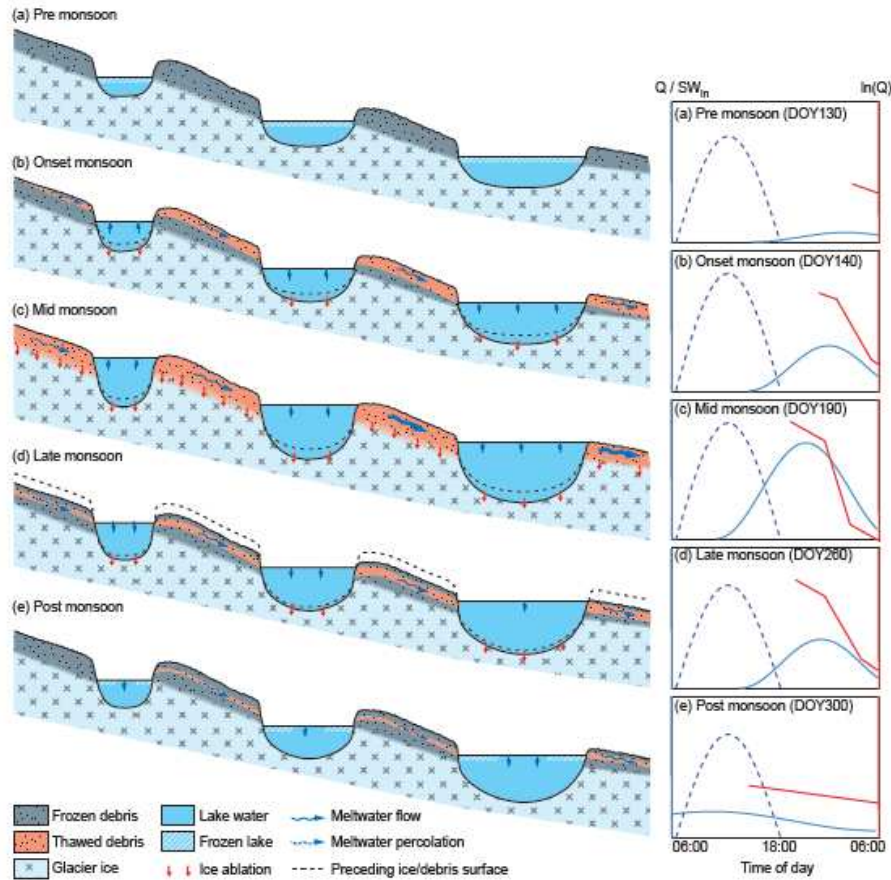
## 192 **4 Discussion**

193 Our results from Khumbu Glacier indicate a hydrological configuration with both similarities  
 194 and distinct differences to those typically reported for Alpine glacier systems in Europe and

195 elsewhere. Systematic progression in timing of peak Q, seasonal undulation in diurnal discharge  
196 amplitude, diurnal hydrograph asymmetry, and clear patterns in hydrograph classification are  
197 commonly described for temperate, debris-free alpine glaciers [e.g. *Richards et al.*, 1996;  
198 *Hannah et al.*, 2000; *Swift et al.*, 2005; *Jobard and Dzikowski*, 2006]. Typically, as the snowline  
199 recedes upglacier and melt season advances, peak Q occurs progressively closer to the time of  
200 heightened  $SW_{in}$  and  $T_a$  and, even for large south-facing valley glaciers such as Aletschgletscher,  
201 equivalent in size to Khumbu Glacier, Q lags the meteorological drivers of melt by <5 hrs during  
202 much of the ablation season [e.g. *Lang*, 1973; *Verbunt et al.*, 2003]. As ablation continues on  
203 debris-free glaciers, the amplitude of Q increases, and the hydrograph form becomes more  
204 accentuated. Here, particularly prior to DOY230 (Figures 3f-h), the patterns of hydrograph  
205 characteristics resemble those reported for temperate alpine settings.

206 However, in contrast to debris-free alpine counterparts, the timing of daily peak and minimum  
207 discharge at Khumbu Glacier shows a more marked delay relative to meteorological drivers of  
208 ablation: peak Q occurs  $\geq 6$  hours after maximum  $SW_{in}$  and  $T_a$ , while minimum Q commonly  
209 coincides with peak irradiance. Q lagging energy fluxes reflects the delay in energy transfers that  
210 initiate melt, particularly for those associated with exchange at the atmosphere-debris interface  
211 and through the debris layer [*Carenzo et al.*, 2016] (Figure 2b). Further lags may relate to  
212 meltwater transit to the monitoring site. Transition in lag time between  $T_a$  and Q mid-season is  
213 ascribed to changes in weather systems and lapse rates reported for the region during the  
214 monsoon [e.g. *Shea et al.*, 2015b, *Steiner and Pellicciotti* 2016], the reduction in both  $T_a$  and  
215  $SW_{in}$ , and subtle changes in the hydrological function of the drainage system. The lack of  
216 association between Q and precipitation has been observed elsewhere on debris-covered glaciers  
217 [e.g. *Thayyen et al.*, 2005]. However, the elongated diurnal hydrograph recession diverges  
218 notably from other glacial observations and more specifically recession data reported here  
219 evidence neither ‘fast’ supraglacial and ‘moderate’ en- and sub-glacial drainage flowpaths,  
220 superimposed on a ‘slow’ persistent baseflow on a diurnal basis, nor a seasonal decline in  
221 recession storage constants [cf. *Gurnell*, 1993]. Furthermore, the gauging station elevation (4930  
222 m a.s.l.), ensures the Q record solely relates to the supraglacial (debris-covered) and shallow  
223 englacial environment. Observations during 2014 confirmed that some supraglacial meltwaters  
224 entered a shallow englacial network, potentially allowing flow between supraglacial ponds,  
225 evidenced by spatial variability in pond turbidity which suggested hydrological connectivity

226 (Figure 1e) [see *Takeuchi et al.*, 2012]. While geomorphic signatures suggested that meltwater  
227 that had once drained or followed seepage pathways through other moraine breach locations,  
228 contemporary field observations indicate these are relict inactive features (IAOs: Fig. 1c).  
229 Consequently, we discuss our data in the context of a conceptual model of the dominantly  
230 supraglacial drainage system illustrated in Figure 3, comprising a debris layer punctuated by a  
231 cascade of lakes or ponds.



232 **Figure 3:** Conceptual model of the seasonal hydrological development of the surface of a  
 233 Himalayan debris-covered glacier over an annual cycle. Indicative daily hydrometeorological  
 234 plots for each stage are shown with  $SW_{in}$  (dashed),  $Q$  (blue), and a natural logarithmic  
 235 transformed  $Q$  used to identify the recession components (red). Pre-monsoon (a) the surface is  
 236 frozen following the winter period, but as the monsoon season approaches (b), the debris-cover  
 237 begins to thaw, and water derived from melting intra-clast ice and ponds commences flow and  
 238 thermal ablation at the base of ponds. Mid monsoon (c) the debris is fully thawed, ponds become  
 239 connected and glacier ice melt occurs and ponds deepen through thermal ablation, which,  
 240 coupled with monsoon rainfall, leads to more efficient drainage over the glacier ice surface.  
 241 Towards the end of the monsoon season (d) the air temperatures drop and initiate freezing at the  
 242 debris surface, while reductions in water flow facilitate upward freezing at the base of the debris  
 243 layer; however, the thawed portion of the debris layer still transfers meltwater from ponds  
 244 towards the glacier margin, albeit delayed. Post monsoon (e), which aligns with the latter portion

245 of our records, continued freeze-up of the lake and debris layer occurs restricting any  
246 transmission of meltwater as winter approaches and the glacier-wide hydrological system drains.

247

248 The cascade of developing ponds represents a series of reservoirs capable of temporarily storing  
249 meltwater and delaying its transit downstream. Combining the pre-monsoon pond areas ( $\sim$   
250  $2.5 \times 10^5 \text{ m}^2$ ; Figure 1) with observation of the outflow lake level varying by  $\sim 0.7 \text{ m}$  over a  
251 diurnal melt cycle, we estimate the supraglacial pond cascade on Khumbu Glacier to account for  
252 a minimum daily storage capacity of  $\sim 1.75 \times 10^5 \text{ m}^3$  (equivalent to 23% of the observed mean  
253 daily discharge). Supported by evidence of progressive pond deepening during the monsoon  
254 season [e.g. *Watson et al.*, 2017a] we conclude that the diurnal storage capacity of the pond  
255 system alone, not including the porous debris layer, can readily accommodate the observed daily  
256 mean P ( $\sim 1.23 \times 10^5 \text{ m}^3$  over the whole glacier area). The timing and magnitude of on-glacier  
257 storage may also be controlled by freeze-thaw processes, analogous to a periglacial environment  
258 given the local permafrost limit. During the winter, both the supraglacial debris layer and ponds  
259 are largely frozen, likely becoming impermeable and unable to convey any surface meltwater. As  
260 the monsoon season develops, the system progressively thaws [e.g. *Sakai et al.*, 2000; *Benn et*  
261 *al.*, 2001; *Namara et al.*, 2017; *Miles et al.*, 2016; *Watson et al.*, 2017a]. The ponds may become  
262 hydrologically linked by three key flowpaths: those within the debris-covered mantle; shallow  
263 debris-filled crevasses [e.g. *Benn et al.*, 2012; *Gulley and Benn*, 2007] or channels formed from  
264 collapsed near-surface englacial conduits [*Miles et al.*, 2017b]; or debris- or water-choked near-  
265 surface passages [*Watson et al.*, 2017a]. Published figures for heterogeneous debris indicate  
266 permeability of between  $10^{-2}$  to  $10^{-6} \text{ m s}^{-1}$  [*Parriaux and Nicoud*, 1990; *Muir et al.*, 2011; *Woo*  
267 *and Steer*, 1983; *Gulley and Benn*, 2007] although mobilization of fines may further reduce  
268 hydraulic efficiency [*Woo and Xia*, 1995]. When thawed, therefore, we anticipate the debris  
269 layer and associated supraglacial and shallow or collapsed englacial features may act as a depth-  
270 limited, transient storage reservoir, regulating bulk meltwater discharge over the glacier surface  
271 and between ponds and hence moderating the overall diurnal flow variance. The debris layer is  
272 underlain by glacier ice with discrete, spatially limited, shallow englacial flowpaths analogous to  
273 continuous permafrost with isolated, closed talik. The result, in the monsoon-influenced climate,  
274 is a thermal regime dominated by the seasonal freezing and thawing of the debris layer, as is



275 evident in our  $T_d$  time-series, and for which the correlations between  $T_a$  and  $T_d$  (Figure 2e) likely  
276 reflect change in debris heat capacity with water content. Khumbu Glacier's supraglacial debris  
277 layer may therefore be considered equivalent to a seasonally cryotic active layer [Bonnaventure  
278 and Lamoureux, 2013].

279 As the monsoon season progresses, evolution of the debris mantle hydrological system may  
280 result in increased inter-pond connectivity. Progressive thaw at depth in the debris layer and  
281 glacier ice melt, despite enlarging the supraglacial storage capacity, also aids the development of  
282 increasingly efficient supra-permafrost drainage: inter-clast ice is replaced with water flow  
283 pathways and increased hydraulic permeability [Woo and Steer, 1983; Woo and Xia, 1995],  
284 providing more efficient connections through the debris and facilitating debris-ice interface and  
285 englacial flowpath development [Gulley and Benn, 2007; Gulley et al., 2009; Miles et al., 2017b;  
286 Watson et al., 2017a]. Strengthening connectivity increases the rapidity of runoff through the  
287 cascading pond system. Sporadic activation, modification or abandonment of flowpaths and  
288 diurnal or seasonal variation in supraglacial pond storage capacity likely contributes to the  
289 observed variation of discharge recession (Fig. 3i). Such delay, peak flow suppression and  
290 attenuated recession, as seen in our data, are indicative of level-pool routing controlling  
291 meltwater transfer through a series of reservoirs [Montaldo et al., 2004] and, as such, the ponds  
292 may be conceptualized as thermokarst [Kirkbride, 1993].

293 Evidence for this role of supraglacial ponds and debris as regulators of meltwater discharge is  
294 exemplified by the diurnal hydrograph recession. When pond levels are at their peak or minima  
295 at seasonal and diurnal time-scales,  $K_P$  and  $K_B$  are determined by the hydraulic conductivity of  
296 the (thawed) debris that separates the individual pond basins.  $K_P$  was not clearly associated with  
297 either  $T_a$  or  $SW_{in}$  nor with daily maximum discharge; the recession segment was not associated  
298 with the magnitude of meltwater production. Once daily meltwater provision declines or ceases,  
299 changes in hydraulic head drive drainage through the pond cascade and the major recession ( $K_R$ )  
300 is governed by outflow channel geometry rather than rates of inflow controlled by debris  
301 permeability.  $K_R$  remains broadly consistent over the hydrologically active period (DOY134-  
302 270). Subsequently, particularly as  $T_a$  and  $T_d$  both fall and water drains from the pond cascade,  
303 water within the debris layer and debris-rich hydraulic connections between ponds refreezes, and

304 the hydraulic efficiency of the system declines. This change is highlighted by  $K_R > K_B$ , the post-  
305 monsoon increase in  $K_R$  and a strongly negative, non-linear relationship between  $K_R$  and peak  $Q$ .

306 The observations following DOY 230 of declining  $Q$  despite positive  $T_a$  and  $T_d$  and precipitation  
307 contributions are counterintuitive. However, given our hydrological analysis and conceptual  
308 model it seems reasonable to suggest that this effect could have arisen from the fully thawed  
309 debris layer readily storing excess water produced in this period and mobilization of fines  
310 impinging on hydrological efficacy, with a consequent net reduction in throughflow evidenced  
311 by gradual increases in all  $K$ -values. The drainage of meltwater continued for  $\sim 45$  days after  
312 night time  $T_a$  dropped to freezing, with around 7% of the observed runoff volume being  
313 delivered in this late- and post-monsoon period. This protracted drainage corresponds well to the  
314 delay in runoff thought to relate to hysteresis caused by a deep groundwater system in the Nepal  
315 Himalaya [Andermann *et al.*, 2012]. Our data suggest that widespread supraglacial debris layers  
316 themselves may contribute to the observations of reservoir behavior in glacierized catchments at  
317 a seasonal timescale, and extend the duration of glacier meltwater delivery to downstream  
318 environments.

## 319 **5 Conclusions**

320 We have demonstrated that the evolving system of supraglacial ponds and accompanying debris  
321 has the capacity to act as a fundamental modulator of proglacial discharge regimes at Khumbu  
322 Glacier. Although there is uncertainty in the causal associations between glacier surface gradient,  
323 debris cover and pond occurrence [Salerno *et al.*, 2017], supraglacial ponds are reported to be  
324 increasingly prevalent on debris-covered glaciers and represent an active and dynamic  
325 hydrological system [Miles *et al.*, 2017a,b; Narama *et al.*, 2017; Watson *et al.*, 2016, 2017a].  
326 Recently, there has been growing recognition that small changes in hydrological function in  
327 mountain regions can have substantial impacts on freshwater availability [e.g. Pritchard, 2017]  
328 and biodiversity [Jacobsen *et al.*, 2012] in terrestrial water bodies and ecosystems in the  
329 Himalaya [Xu *et al.*, 2009; Salerno *et al.*, 2016]. To understand the hydrological response of  
330 debris-covered glaciers and to forecast changes in water resources and ecosystem services in the  
331 region, it is crucial to explicitly incorporate processes relating to the thermodynamics and  
332 hydrology of widespread debris mantles that can now be considered as cryotic, thermokarstic  
333 active layers – systems that are more commonly described solely in periglacial settings

334 [Bonnaventure and Lamoureux, 2013]. Further geophysical and hydrochemical exploration of  
335 debris cover [e.g. Muir *et al.*, 2011; McCarthy *et al.*, 2017] is needed to better define the nature  
336 of the supraglacial debris-covered drainage system and the modes and thermodynamics of  
337 hydraulic connectivity between ponds. With ~75 to 90% glacier area in the Himalaya above  
338 4500–5000 m a.s.l., the elevation range commonly associated with the regional permafrost limit  
339 [Schmidt *et al.*, 2015], processes we describe here should be widely applicable throughout the  
340 region and highlight the important role that debris-layer supraglacial hydrology may have on  
341 mediating glacier runoff characteristics in High Mountain Asia. Long-term increases in areal  
342 extent of debris cover and ponds will not only contribute to more rapid glacier mass loss but, we  
343 propose, also alter patterns of meltwater supply and quality to downstream catchments through  
344 their roles as temporary reservoirs and flow regulators. A more complete understanding of this  
345 buffering process is crucial to improving projections of the region’s future water resources in a  
346 changing climate.

347

### 348 **Acknowledgments and Data**

349 All authors acknowledge the Royal Society (Research Grant: RG120393) and the British Society  
350 for Geomorphology. Summit Treks provided logistical support in Nepal. Patrick Wagnon kindly  
351 provided incident radiation and precipitation data. TDI, PRP, NFG and JWB led the analysis,  
352 writing and conceptual development. TDI, AVR, DJQ and MJG undertook fieldwork in Nepal.  
353 PRP provided fieldwork equipment and instruments. CSW acquired and processed supraglacial  
354 lake data. All authors contributed to development, editing and revision of the final manuscript.  
355 We thank the two reviewers who both provided insightful suggestions to help improve the paper.

356 All new data presented here are available via [www.pangaea.de](http://www.pangaea.de) :

357 [doi.org/10.1594/PANGAEA.883071](https://doi.org/10.1594/PANGAEA.883071) and [doi.org/XXXXXXX](https://doi.org/XXXXXXX)

358

### 359 **References**

360 Andermann, C., L. Longuevergne, S. Bonnet, A. Crave, P. Davy and R. Gloaguen (2012). Impact  
361 of transient groundwater storage on the discharge of Himalayan rivers. *Nature*  
362 *Geoscience*, 5, 127-132.

- 363 Bajracharya, S.R, S.B. Maharjan, F. Shrestha, W. Guo, S. Liu, W. Immerzeel and B. Shrestha  
364 (2015). The glaciers of the Hindu Kush Himalayas: current status and observed changes  
365 from the 1980s to 2010. *International Journal of Water Resources Development*, 31, 161-  
366 173.
- 367 Basnett, S., A.V. Kulkarni, and T. Bolch (2013). The influence of debris cover and glacial lakes  
368 on the recession of glaciers in Sikkim Himalaya, India. *Journal of Glaciology*, 59, 1035-  
369 1046.
- 370 Benn, D.I., T. Bolch, K. Hands, J. Gulley, A. Luckman, L.I. Nicholson, D. Quincey, S.  
371 Thompson, R. Toumi and S. Wiseman (2012). Response of debris-covered glaciers in  
372 the Mount Everest region to recent warming, and implications for outburst flood hazards.  
373 *Earth-Science Reviews*, 114, 156-174.
- 374 Benn, D.I., S. Wiseman, and K.A. Hands (2001). Growth and drainage of supraglacial lakes on  
375 debris mantled Ngozumpa Glacier, Khumbu Himal, Nepal. *Journal of Glaciology*, 47,  
376 626-638.
- 377 Bhatt, M.P., N. Takeuchi and M.F. Acevedo (2016). Chemistry of Supraglacial Ponds in the  
378 Debris-Covered Area of Lirung Glacier in Central Nepal Himalayas. *Aquatic*  
379 *Geochemistry*, 22(1), pp.35-64.
- 380 Bolch, T., M. Buchroithner, T. Pieczonka and A. Kunert (2008). Planimetric and volumetric  
381 glacier changes in the Khumbu Himal, Nepal, since 1962 using Corona, Landsat TM and  
382 ASTER data. *Journal of Glaciology*, 54, 592-600.
- 383 Bolch, T., A. Kulkarni, A. Kääb, C. Huggel, F. Paul, J.G. Cogley, H. Frey, J.S. Kargel, K. Fujita,  
384 M. Scheel and S. Bajracharya (2012). The state and fate of Himalayan glaciers. *Science*,  
385 336, 310-314.
- 386 Bonnaventure, P.P. and S.F. Lamoureux (2013). The active layer: A conceptual review of  
387 monitoring, modelling techniques and changes in a warming climate. *Progress in*  
388 *Physical Geography*, 37, 352-376.
- 389 Bookhagen, B. and D.W. Burbank (2010). Toward a complete Himalayan hydrological budget:  
390 Spatiotemporal distribution of snowmelt and rainfall and their impact on river  
391 discharge. *Journal of Geophysical Research: Earth Surface*, 115(F3), F03019.
- 392 Brun, F., E. Berthier, P. Wagnon, A. Kääb, D. Treichler, H.B. Franz, A.C. McAdam, D.W.  
393 Ming, C. Freissinet, P.R. Mahaffy and D.L. Eldridge (2017). A spatially resolved  
394 estimate of High Mountain Asia glacier mass balances from 2000 to 2016. *Nature*  
395 *Geoscience*. doi:10.1038/ngeo2999
- 396 Brun, F., P. Buri, E.S. Miles, P. Wagnon, J. Steiner, E. Berthier, S. Ragettli, P. Kraaijenbrink,  
397 W.W. Immerzeel and F. Pellicciotti (2016). Quantifying volume loss from ice cliffs on  
398 debris-covered glaciers using high-resolution terrestrial and aerial photogrammetry.  
399 *Journal of Glaciology*, 62, 684-695.
- 400 Carenzo, M., F. Pellicciotti, J. Mabillard, T. Reid and B.W. Brock (2016). An enhanced  
401 temperature index model for debris-covered glaciers accounting for thickness effect.  
402 *Advances in Water Resources*, 94, 457-469.

- 403 Di Baldassarre, G. and A. Montanari (2009). Uncertainty in river discharge observations: a  
404 quantitative analysis. *Hydrology and Earth System Sciences*, 13(6), 913-921. DOI:  
405 10.5194/hess-13-913-2009
- 406 Evatt, G.W., I.D. Abrahams, M. Heil, C. Mayer, J. Kingslake, S.L. Mithcel, A.C. Flower and  
407 C.D. Clark (2015). Glacial melt under a porous debris layer. *Journal of Glaciology*. 61,  
408 825-836.
- 409 Fujita, K. and A. Sakai (2014). Modelling runoff from a Himalayan debris-covered glacier.  
410 *Hydrology and Earth System Sciences*, 18, 2679–2694.
- 411 Gades, A., H. Conway, N. Nereson, N. Naito and T. Kadota. (2000). Radio echo-sounding  
412 through supraglacial debris on Lirung and Khumbu Glaciers, Nepal Himalayas. *IAHS*  
413 *Publication*, 264, 13-24.
- 414 Gardelle, J., Y. Arnaud and E. Berthier (2011). Contrasted evolution of glacial lakes along the  
415 Hindu Kush Himalaya mountain range between 1990 and 2009. *Global and Planetary*  
416 *Change*, 75, 47-55 (2011).
- 417 Gulley, J. and D.I. Benn (2007). Structural control of englacial drainage systems in Himalayan  
418 debris-covered glaciers. *Journal of Glaciology*, 53, 399-412.
- 419 Gulley, J.D., D.I. Benn, D. Müller and A. Luckman (2009). A cut-and-closure origin for  
420 englacial conduits in uncrevassed regions of polythermal glaciers. *Journal of Glaciology*,  
421 55, 66-80.
- 422 Gurnell A.M. (1993). How many reservoirs? An analysis of flow recessions from a glacier basin.  
423 *Journal of Glaciology* 39, 132-134.
- 424 Hannah, D.M., B.P. Smith, A.M. Gurnell and G.R. McGregor (2000). An approach to  
425 hydrograph classification. *Hydrological Processes*, 14, 317-338.
- 426 Herschy, R.W., 1995. Streamflow measurement. CRC Press.
- 427 Hodgkins, R., R. Cooper, M. Tranter and J. Wadham (2013). Drainage system development in  
428 consecutive melt seasons at a polythermal, Arctic glacier, evaluated by flow recession  
429 analysis and linear reservoir simulation. *Water Resources Research*, 49, 4230-4243.
- 430 Hudson, R. and J. Fraser (2005). The mass balance (or dry injection) method. *Streamline*  
431 *Watershed Management Bulletin*, 9, 6-12.
- 432 Immerzeel, W.W. and M.F.P. Bierkens (2012). Asia's water balance. *Nature Geoscience*, 5, 841-  
433 842.
- 434 Immerzeel, W.W., L.P.H. Van Beek and M.F.P. Bierkens (2010) Climate change will affect the  
435 Asian water towers. *Science*, 328, 1382–1385.
- 436 Immerzeel, W.W., L.P.H. Van Beek, M. Konz, A.B. Shrestha and M.F.P. Bierkens (2012).  
437 Hydrological response to climate change in a glacierized catchment in the Himalayas.  
438 *Climatic Change*, 110, 721-736..
- 439 Jacobsen, D., A.M. Milner, L.E. Brown and O. Dangles (2012). Biodiversity under threat in  
440 glacier-fed river systems. *Nature Climate Change*, 2, 361-364.

- 441 Jobard, S. and M. Dzikowski (2006). Evolution of glacial flow and drainage during the ablation  
442 season. *Journal of Hydrology*, 330, 663-671.
- 443 Kääh, A., E. Berthier, C. Nuth, J. Gardelle and Y. Arnaud (2012) Contrasting patterns of early  
444 twenty-first-century glacier mass change in the Himalayas. *Nature*, 488, 495-498.
- 445 King, O., D.J. Quincey, J.L. Carrivick and A.V. Rowan (2017). Spatial variability in mass loss of  
446 glaciers in the Everest region, central Himalayas, between 2000 and 2015. *The  
447 Cryosphere*, 11, 407-426.
- 448 Kirkbride, M.P. (1993). The temporal significance of transitions from melting to calving termini  
449 at glaciers in the central Southern Alps of New Zealand. *The Holocene*, 3, 232-240.
- 450 Lang, H. (1973). Variations in the relation between glacier discharge and meteorological  
451 elements. *IAHS Publication*, 95, 85-96.
- 452 Lutz, A. F., W.W. Immerzeel, A.B. Shrestha and M.F.P. Bierkens (2014). Consistent increase in  
453 High Asia's runoff due to increasing glacier melt and precipitation. *Nature Climate  
454 Change*, 4, 587-592.
- 455 McCarthy, M., H. Pritchard, I. Willis and E. King (2017). Ground-penetrating radar  
456 measurements of debris thickness on Lirung Glacier, Nepal. *Journal of Glaciology*, 63,  
457 543-555.
- 458 Mae, S., H. Wushiki, Y. Ageta and K. Higuchi (1975). Thermal drilling and temperature  
459 measurements in Khumbu Glacier, Nepal Himalayas. *Seppyo*, 37, 161-169.
- 460 Mertes, J.R., S.S. Thompson, A.D. Booth, J.D. Gulley and D.I. Benn (2017). A conceptual  
461 model of supra-glacial lake formation on debris-covered glaciers based on GPR facies  
462 analysis. *Earth Surface Processes and Landforms*, 42, 903-914.
- 463 Miles, E.S., F. Pellicciotti, I.C. Willis, J.F. Steiner, P. Buri and N.S. Arnold (2016). Refined  
464 energy-balance modelling of a supraglacial pond, Langtang Khola, Nepal. *Annals of  
465 Glaciology*, 57, 29-40.
- 466 Miles, E.S., I.C. Willis, N.S. Arnold, J. Steiner and F. Pellicciotti (2017a). Spatial, seasonal and  
467 interannual variability of supraglacial ponds in the Langtang Valley of Nepal, 1999–  
468 2013. *Journal of Glaciology*, 63, 88-105.
- 469 Miles, E.S., J. Steiner, I. Willis, P. Buri, W.W. Immerzeel, A. Chesnokova, and F. Pellicciotti  
470 (2017b). Pond Dynamics and Supraglacial-Englacial Connectivity on Debris-Covered  
471 Lirung Glacier, Nepal. *Frontiers in Earth Science*, 5, 69.
- 472 Montaldo, N., M. Mancini and R. Rosso (2004). Flood hydrograph attenuation induced by a  
473 reservoir system: analysis with a distributed rainfall-runoff model. *Hydrological  
474 Processes*, 18, 545-563.
- 475 Muir, D.L., M. Hayashi and A.F. McClymont (2011). Hydrological storage and transmission  
476 characteristics of an alpine talus. *Hydrological Processes*, 25, 2954-2966.
- 477 Narama, C., M. Daiyrov, T. Tadono, M. Yamamoto, A. Kääh, R. Morita and J. Ukita (2017).  
478 Seasonal drainage of supraglacial lakes on debris-covered glaciers in the Tien Shan  
479 Mountains, Central Asia. *Geomorphology*, 286, 133-142.

- 480 Nuimura, T., K. Fujita, K. Fukui, K. Asahi, R. Aryal and Y. Ageta (2011). Temporal changes in  
481 elevation of the debris-covered ablation area of Khumbu Glacier in the Nepal Himalaya  
482 since 1978. *Arctic, Antarctic, and Alpine Research*, 43, 246-255.
- 483 Østrem, G. (1959). Ice melting under a thin layer of moraine, and the existence of ice cores in  
484 moraine ridges. *Geografiska Annaler*, 41, 228-230.
- 485 Parriaux, A., and G.F. Nicoud (1990). Hydrological behaviour of glacial deposits in mountainous  
486 areas. *IAHS Publication* 190, 291-312.
- 487 Pritchard, H.D., 2017. Asia's glaciers are a regionally important buffer against  
488 drought. *Nature*, 545(7653), 169-174.
- 489 Quincey, D.J., S.D. Richardson, A. Luckman, R.M. Lucas, J.M. Reynolds, M.J. Hambrey and  
490 N.F. Glasser (2007). Early recognition of glacial lake hazards in the Himalaya using  
491 remote sensing datasets. *Global and Planetary Change*, 56, 137-152.
- 492 Ragetti, S., F. Pellicciotti, W.W. Immerzeel, E.S. Miles, L. Petersen, M. Heynen, J.M. Shea, D.  
493 Stumm, S. Joshi and A. Shrestha (2015). Unraveling the hydrology of a Himalayan  
494 catchment through integration of high resolution in situ data and remote sensing with an  
495 advanced simulation model. *Advances in Water Resources*, 78, 94-111.
- 496 Rantz, S.E., and others (1982). Measurement and computation of streamflow: Volume 2.  
497 Computation of discharge. USGS Water Supply Paper 2175. USGPO, 285-631.
- 498 Reynolds, J.M. (2000). On the formation of supraglacial lakes on debris-covered glaciers. *IAHS*  
499 *Publication*, 264, 153-164.
- 500 Richards, K., M. Sharp, N. Arnold, A. Gurnell, M. Clark, M. Tranter, P. Nienow, G. Brown, I.  
501 Willis and W. Lawson (1996). An integrated approach to modelling hydrology and water  
502 quality in glacierized catchments. *Hydrological Processes*, 10, 479-508.
- 503 Rowan, A.V., D.L. Egholm, D.J. Quincey and N.F. Glasser (2015). Modelling the feedbacks  
504 between mass balance, ice flow and debris transport to predict the response to climate  
505 change of debris-covered glaciers in the Himalaya, *Earth and Planetary Science Letters*,  
506 430, 427-438.
- 507 Sakai, A., K. Fujita, T. Aoki, K. Asahi, and M. Nakawo (1997). Water discharge from the Lirung  
508 Glacier in Langtang Valley, Nepal Himalayas, 1996. *Bulletin of Glacier Research* 15, 79-  
509 83.
- 510 Sakai, A., M. Nakawo and K. Fujita (2002). Distribution characteristics and energy balance of  
511 ice cliffs on debris-covered glaciers, Nepal Himalaya. *Arctic, Antarctic, and Alpine*  
512 *Research*, 34, 12-19.
- 513 Sakai, A., N. Takeuchi, K. Fujita and M. Nakawo (2000). Role of supraglacial ponds in the  
514 ablation process of a debris-covered glacier in the Nepal Himalayas. *IAHS Publication*,  
515 264, 119-132.
- 516 Salerno, F., M. Rogora, R. Balestrini, A. Lami, G.A. Tartari, S. Thakuri, D. Godone, M. Freppaz  
517 and G. Tartari (2016). Glacier melting increases the solute concentrations of Himalayan  
518 glacial lakes. *Environmental Science & Technology*, 50, 9150-9160.

- 519 Salerno, F., S. Thakuri, G. Tartari, T. Nuimura, S. Sunako, A. Sakai, K. Fujita. 2017. Debris-  
520 covered glacier anomaly? Morphological factors controlling changes in the mass balance,  
521 surface area, terminus position, and snow line altitude of Himalayan glaciers. *Earth and*  
522 *Planetary Science Letters*, 471, 19-31.
- 523 Scherler, D., B. Bookhagen and M.R. Strecker (2011). Spatially variable response of Himalayan  
524 glaciers to climate change affected by debris cover. *Nature Geoscience*, 4, 156-159.
- 525 Schmid, M.O., P. Baral, S. Gruber, S. Shahi, T. Shrestha, D. Stumm and P. Wester (2015).  
526 Assessment of permafrost distribution maps in the Hindu Kush Himalayan region using  
527 rock glaciers mapped in Google Earth. *The Cryosphere*, 9, 2089-2099.
- 528 Shea, J.M., W.W. Immerzeel, P. Wagnon, C. Vincent and S. Bajracharya (2015a). Modelling  
529 glacier change in the Everest region, Nepal Himalaya. *The Cryosphere*, 9, 1105-1128.
- 530 Shea J.M., P. Wagnon, W.W. Immerzeel, R. Biron, F. Brun and F. Pellicciotti. (2015b). A  
531 comparative high-altitude meteorological analysis from three catchments in the Nepalese  
532 Himalaya, *International Journal of Water Resources Development*, 31, 174-200.
- 533 Sherpa, S.F., P. Wagnon, F. Brun, E. Berthier, C. Vincent, Y. Lejeune, Y. Arnaud, R.B.  
534 Kayastha and A. Sinisolo (2017). Contrasted surface mass balances of debris-free  
535 glaciers observed between the southern and the inner parts of the Everest region (2007–  
536 15). *Journal of Glaciology*, XX, 1-15. doi: 10.1017/jog.2017.30
- 537 Soncini, A., D. Bocchiola, G. Confortola, U. Minora, E. Vuillermoz, F. Salerno, G. Viviano, D.  
538 Shrestha, A. Senese, C. Smiraglia, and G. Diolaiuti (2016). Future hydrological regimes  
539 and glacier cover in the Everest region: The case study of the upper Dudh Koshi basin.  
540 *Science of the Total Environment*, 565, 1084-1101. doi: 10.1016/j.scitotenv.2016.05.138
- 541 Steiner, J.F. and F. Pellicciotti (2016). Variability of air temperature over a debris-covered  
542 glacier in the Nepalese Himalaya. *Annals of Glaciology*, 57, 295-307.
- 543 Swift, D.A., P.W. Nienow, T.B. Hoey and D.W. Mair (2005). Seasonal evolution of runoff from  
544 Haut Glacier d'Arolla, Switzerland and implications for glacial geomorphic processes.  
545 *Journal of Hydrology*, 309,133-148.
- 546 Takeuchi, N., A. Sakai, K. Shiro, K. Fujita and N. Masayoshi (2012). Variation in suspended  
547 sediment concentration of supraglacial lakes on debris-covered area of the Lirung Glacier  
548 in the Nepal Himalayas. *Global Environmental Reseach*, 16, 95-104.
- 549 Thakuri, S., F. Salerno, C. Smiraglia, T. Bolch, C. D'Agata, G. Viviano and G. Tartari (2014).  
550 Tracing glacier changes since the 1960s on the south slope of Mt. Everest (central  
551 Southern Himalaya) using optical satellite imagery. *The Cryosphere*, 8, 1297-1315.
- 552 Thayyen, R.J., J.T. Gergan and D.P. Dobhal (2005). Monsoonal control on glacier discharge and  
553 hydrograph characteristics, a case study of Dokriani Glacier, Garhwal Himalaya, India.  
554 *Journal of Hydrology*, 306, 37-49.
- 555 Thompson, S., D.I. Benn, J. Mertes and A. Luckman (2016). Stagnation and mass loss on a  
556 Himalayan debris-covered glacier: processes, patterns and rates. *Journal of Glaciology*,  
557 62, 67-485.



- 558 Verbunt, M., J. Gurtz, K. Jasper, H. Lang, P. Warmerdam, and M. Zappa (2003). The  
559 hydrological role of snow and glaciers in alpine river basins and their distributed  
560 modeling. *Journal of Hydrology*, 282(1), 36-55.
- 561 Vincent, C., P. Wagnon, J.M. Shea, W.W. Immerzeel, P. Kraaijenbrink, D. Shrestha, A. Soruco,  
562 Y. Arnaud, F. Brun, E. Berthier, S.F. Sherpa (2016). Reduced melt on debris-covered  
563 glaciers: investigations from Changri Nup Glacier, Nepal. *The Cryosphere*, 10, 1845-  
564 1858.
- 565 Watson, S. C., D.J. Quincey, J.L. Carrivick and M.W. Smith (2016). The dynamics of  
566 supraglacial water storage in the Everest region, central Himalaya. *Global and Planetary*  
567 *Change*, 142, 14-27.
- 568 Watson, C.S., D.J. Quincey, J.L. Carrivick, M.W. Smith, A.V. Rowan and R. Richardson  
569 (2017a). Heterogeneous water storage and thermal regime of supraglacial ponds on  
570 debris-covered glaciers. *Earth Surface Processes and Landforms* (early view) doi:  
571 10.1002/esp.4236.
- 572 Watson, C.S., D.J. Quincey, J.L. Carrivick and M.W. Smith (2017b). Ice cliff dynamics in the  
573 Everest region of the Central Himalaya. *Geomorphology*, 278, 238-251.
- 574 Wessels, R.L., J.S. Kargel and H.H. Kieffer (2002). ASTER measurement of supraglacial lakes  
575 in the Mount Everest region of the Himalaya. *Annals of Glaciology*, 34, 399-40.
- 576 Woo, M.K. and P. Steer (1983). Slope hydrology as influenced by thawing of the active layer,  
577 Resolute, NWT. *Canadian Journal of Earth Sciences*, 20, 978-986.
- 578 Woo, M.K. and Z. Xia (1995). Suprapermafrost groundwater seepage in gravelly terrain,  
579 Resolute, NWT, Canada. *Permafrost and Periglacial Processes*, 6(1), 57-72.
- 580 Xu, J., R.E. Grumbine, A. Shrestha, M. Eriksson, X. Yang, Y. Wang and A. Wilkes (2009). The  
581 melting Himalayas: cascading effects of climate change on water, biodiversity, and  
582 livelihoods. *Conservation Biology*, 23, 520-530.

Figure 1.

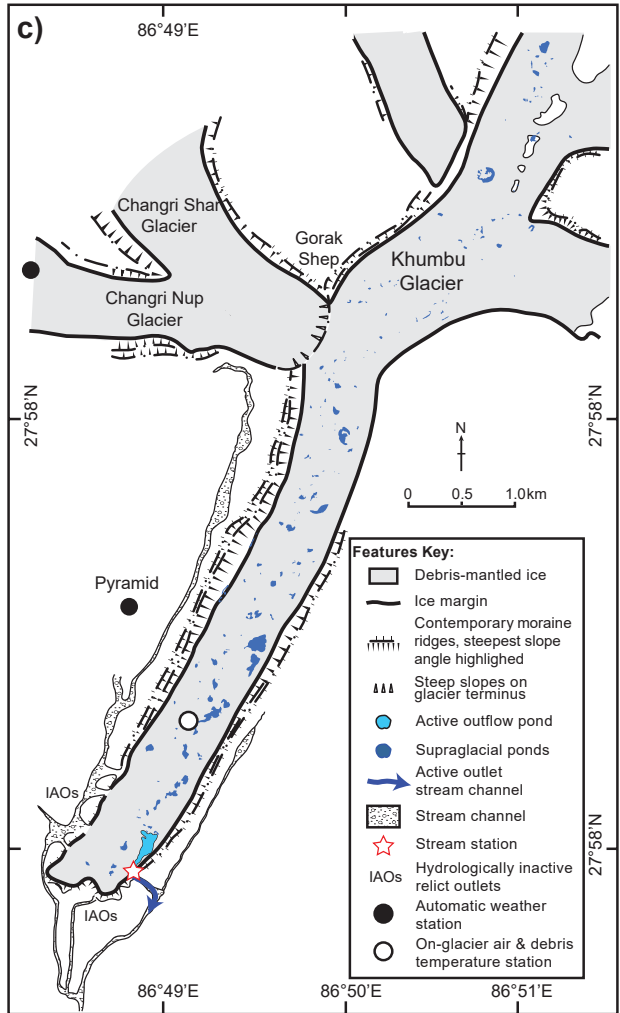
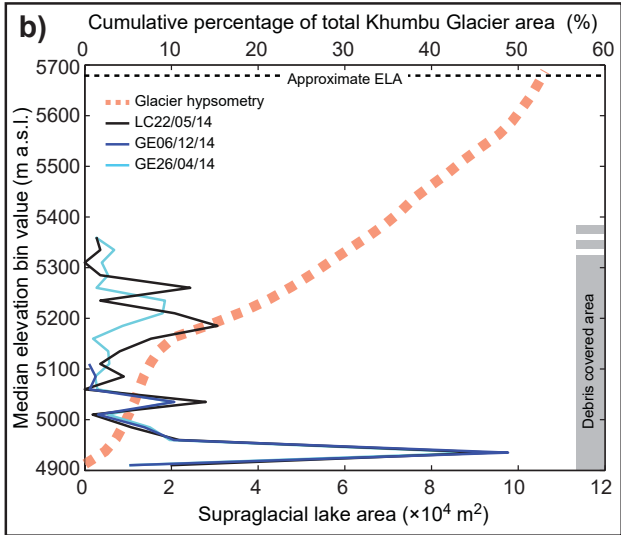
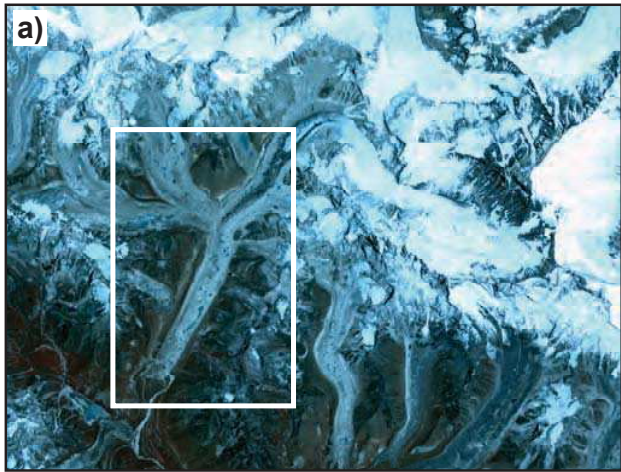


Figure 2.

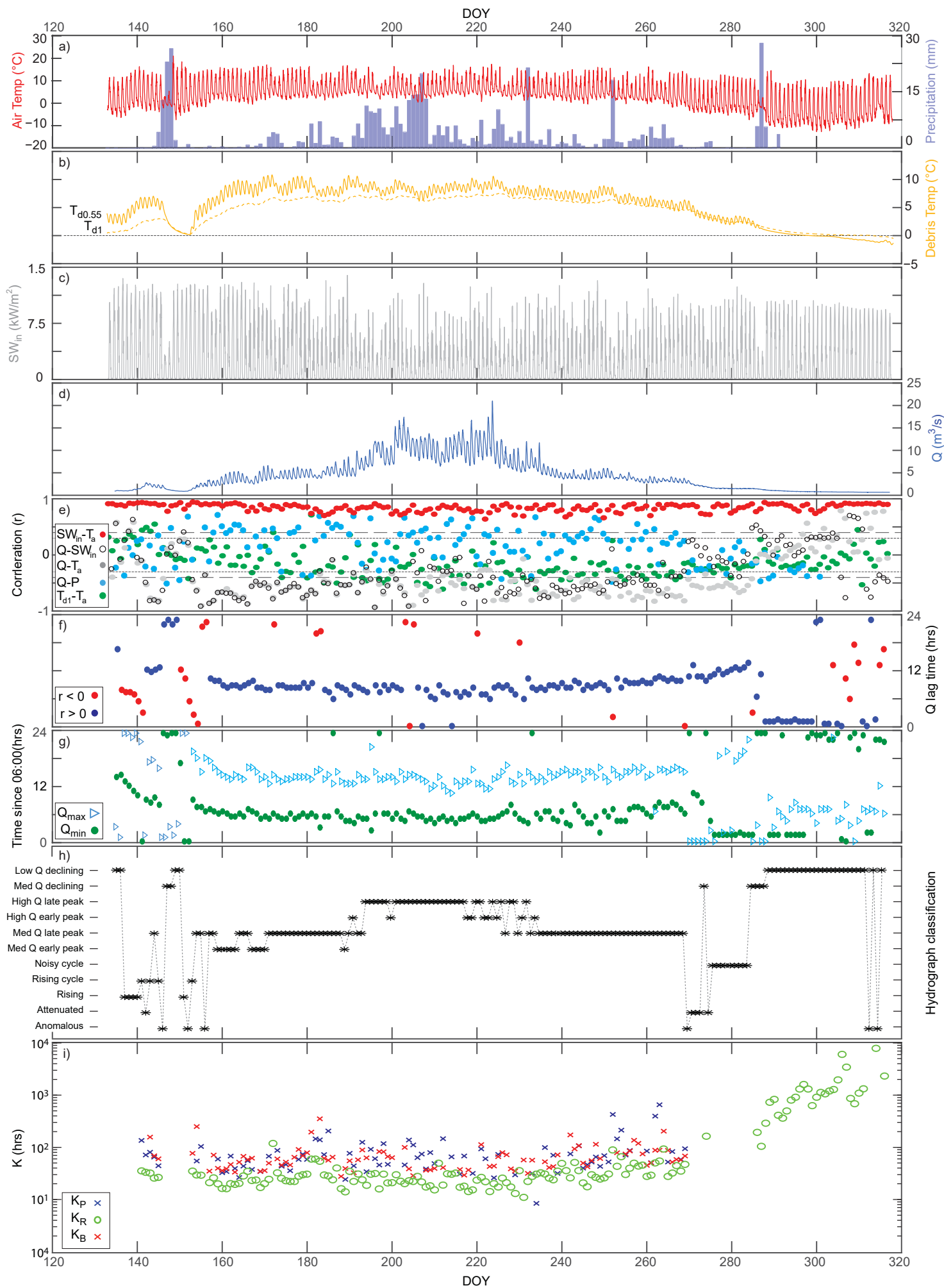
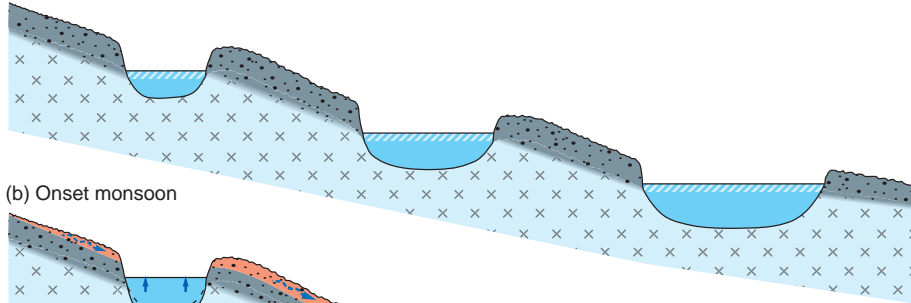
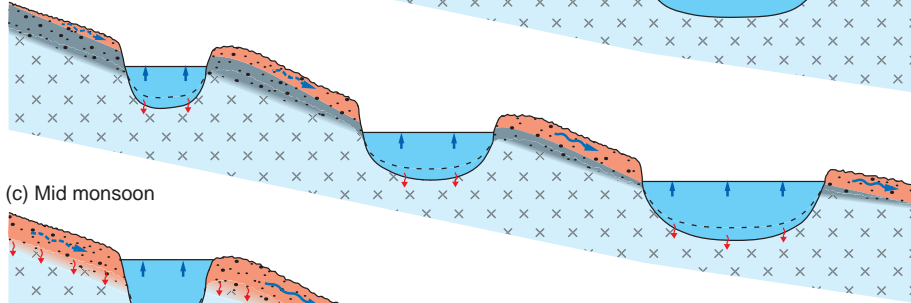


Figure 3.

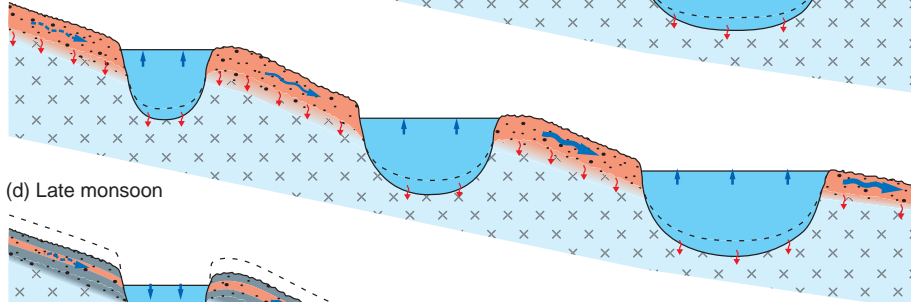
(a) Pre monsoon



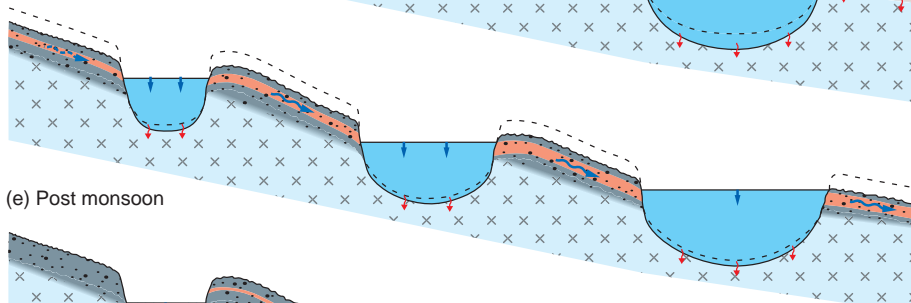
(b) Onset monsoon



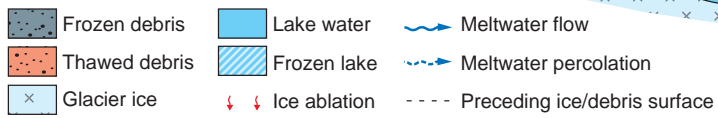
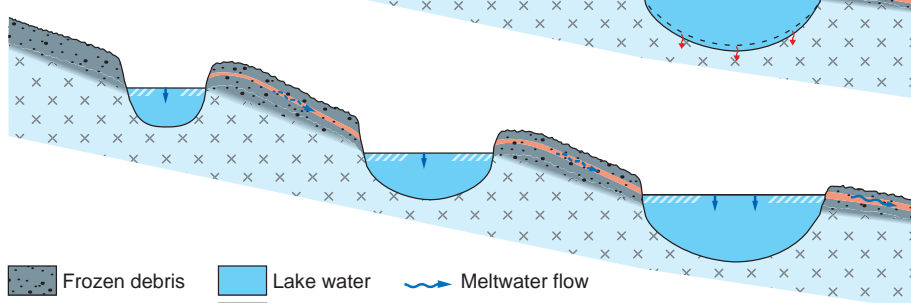
(c) Mid monsoon



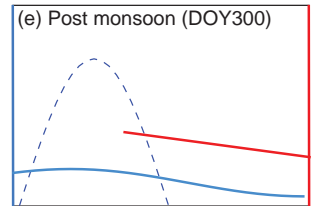
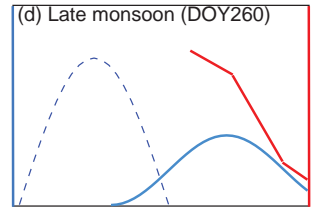
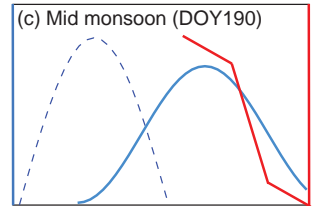
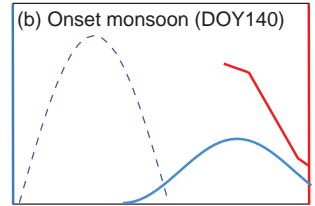
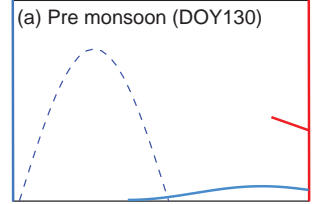
(d) Late monsoon



(e) Post monsoon



$Q / SW_{in}$   $\ln(Q)$



06:00 18:00 06:00  
Time of day